ample good atomic coordinates were only achieved by using r_m values in the range 2·50 to 2·60 Å and 2·40 to 2·60 Å for sodium oxalate and formate respectively. The best agreement for both salts corresponds to r_m = 2·60 Å and in this case an appreciable improvement is obtained with respect to the results given in Table 5 (r_m = 2·50 Å). Because of our limited experience we cannot exclude the possibility that further analyses will lead to a modification of the r_m values of Table 3.

From Tables 5 and 6 it is clear that the best potentials for van der Waals atom–ion and ion–ion interactions are in general those of the rare gases following the alkali metals. It is perhaps significant that the van der Waals radii of the 'best' noble gases are about 1·90, 2·00, 2·20 and 2·40 Å for Ar, Kr, Xe and Rn, corresponding to Slater's ionic radii 1·80, 2·20, 2·35 and 2·60 Å for Na, K, Rb and Cs respectively (Slater, 1965). These last figures agree with the radii of maximum radial charge density in the outermost shell of the alkali metals computed by Liberman, Waber & Cromer (1965) as 1·71, 2·16, 2·29 and 2·52 Å. It is remarkable that the inert gas potentials are qualitatively adequate to describe van der Waals non bonded interactions between S–S, Cl–Cl, Br–Br, I–I, Na^+–Na^+, K^+–K^+, Rb^+–Rb^+ and Cs^+–Cs^+. It seems likely, therefore, that the present approach may be extended to further atoms or ions.

In conclusion we believe that suitable atom–ion and ion–ion potentials are available to locate with sufficient accuracy the minima of the energy surface in crystals in order to solve the phase problem, at least for some simple cases. We propose to extend these calculations to more difficult biological crystal structures thus submitting these functions to a more severe test.

The authors acknowledge the Consiglio Nazionale delle Ricerche for the sponsorship of this work through the Istituto di Chimica delle Macromolecole, Milano.

References

BARTELL, L. S. (1960). *J. Chem. Phys.* **32**, 827.
BAUGHAN, E. C. (1959). *Trans. Faraday Soc.* **55**, 736.
BRAGG, W. L. (1920). *Phil. Mag.* **40**, 169.
CHAKRABORTI, P. K. (1966). *J. Chem. Phys.* **44**, 3137.
DI NOLA, A. & GIGLIO, E. (1970). *Acta Cryst.* A**26**, 144.
GIACOMELLO, P. & GIGLIO, E. (1970). *Acta Cryst.* A**26**, 324.
GIGLIO, E. (1969). *Nature, Lond.* **222**, 339.
GIGLIO, E. (1970). *Z. Kristallogr.* **131**, 385.
GIGLIO, E. & LIQUORI, A. M. (1967). *Acta Cryst.* **22**, 437.
GIGLIO, E., LIQUORI, A. M. & MAZZARELLA, L. (1968). *Nuovo Cim.* **56**B, 57.
International Tables for X-ray Crystallography (1965). Vol. I. Birmingham: Kynoch Press.
JEFFREY, G. A. & PARRY, G. S. (1954). *J. Amer. Chem. Soc.* **76**, 5283.
KANE, G. (1939). *J. Chem. Phys.* **7**, 603.
LEVIN, A. A., SYRKIN, YA. K. & DYATKINA, M. E. (1969). *Russ. Chem. Rev.* **38** (2), 95.
LIBERMAN, D., WABER, J. T. & CROMER, D. T. (1965). *Phys. Rev.* **137**A, 27.
LIQUORI, A. M. (1969). *Quart. Rev. Biophys.* **2**, 65.
MASON, E. A. & RICE, W. E. (1954). *J. Chem. Phys.* **22**, 843.
MILLER, G. A. (1960). *J. Phys. Chem.* **64**, 163.
SLATER, J. C. (1965). *Quantum Theory of Molecules and Solids*, Vol. 2. New York: McGraw-Hill.
WEISS, E. (1963). *Helv. Chim. Acta*, **46**, 2051.
WEISS, E. & BÜCHNER, W. (1963). *Helv. Chim. Acta*, **46**, 1121.
WEISS, E. & BÜCHNER, W. (1964). *Helv. Chim. Acta*, **330**, 251.
ZACHARIASEN, W. H. (1940). *J. Amer. Chem. Soc.* **62**, 1011.

Acta Cryst. (1971). A**27**, 233

The Prediction of Spot Positions on Equi-Inclination Weissenberg Photographs

BY J. A. D. JEFFREYS

Department of Pure and Applied Chemistry, University of Strathclyde, Glasgow C. 1, *Scotland*

(*Received* 6 *July* 1970 *and in revised form* 21 *September* 1970)

An algorithm is presented for using equi-inclination Weissenberg and precession photographs to index an unknown triclinic cell to give a right-handed homogeneous vertex at the origin. Using such indexing, and known crystal parameters and camera settings, the geometry of reflexion is analysed to predict spot positions on both halves of equi-inclination Weissenberg photographs.

Introduction

The method for converting spot positions on a Weissenberg photograph into reciprocal-lattice coordinates has been fully described by Buerger (1942*a*). The converse operation of predicting spot positions on any one of a pack of films recording the intensities of the *n*-layer is treated below. The orientation of the film both in the camera and after development, the camera design, and the axial labelling must be strictly defined if the treatment given is to apply. This assumes that both a Weissenberg and a precession camera are available, and it is limited to equi-inclination Weissenberg photographs.

Apparatus

Film

Before development the film, held flat, is viewed from the side remote from the X-ray source and the top-right corner cut-off. After development, precession and rotation photographs are viewed in this orientation. Weissenberg photographs are viewed in the orientation in which the axial lines run bottom-left to top-right; the snip merely identifies the upper half of the film, and whether it appears top-right or top-left depends on the camera design.

Cameras

In the descriptions that follow, it is assumed that the camera lies between the observer and the X-ray source.

WEISSENBERG

It is assumed that the dial axis is horizontal, and the dial and goniometer head are to the right of the crystal. When the top of the dial moves toward the X-ray source, if the dial reading increases $S1=+1$; if it decreases $S1=-1$. For each film a dial reading is made as the left-hand edge of the record (in its standard orientation) is exposed. When the top of the dial moves toward the X-ray source, if the film is moved to the left then the snip will appear at the top-right corner of the film. [If the cassette is imagined as a nut sliding along a threaded dial axis, then as described above that thread is left-handed. Such coupling has been variously described as left-handed (Peerdeman & Bijvoet, 1956; Stout & Jensen, 1968) and right-handed (Ramaseshan, 1964]. For the sense of rotation described above, if the cassette moves to the right, the snip will appear at the top-left corner of the film. In the standard orientation, the axial sequence across the film is the same for either coupling. The following analysis assumes too that as the equi-inclination angle is increased the dial moves away from the X-ray source, and the slit in the layer-line screen is moved away from the dial. Then the positive direction of the rotation axis extends to the left, and for each layer of data the index along the rotation axis is positive.

PRECESSION

It is assumed that the dial axis is horizontal, that the dial lies to the right of the crystal, and that when the top of the dial moves toward the X-ray source the dial reading increases.

Axial labelling

Conventionally, a triclinic cell is indexed on the Bravais-reduced cell (Azaroff & Buerger, 1958; Kennard, Speakman & Donnay, 1967) which has right-handed axes and a homogeneous vertex at the origin, all the angles being $\geqslant 90°$; *i.e.* an obtuse unit cell. The corresponding reciprocal cell then has all angles $\leqslant 90°$, *i.e.* an acute cell. But when, as with cameras, a crystal is set on morphological evidence, it does not follow that the most obvious or convenient reciprocal cell is acute. The chance that it is so is 50%. That two parallelepipeds with axial lengths (a,b,c), and interaxial angles either (1) (λ,μ,ν), or (2) $(180-\lambda, 180-\mu, 180-\nu)$ are different can be seen comparing their volumes, V_i. Writing C for $(\cos^2\lambda+\cos^2\mu+\cos^2\nu)$, P for $(\cos\lambda\cos\mu\cos\nu)$:

$$V_1=abc(1-C+2P)^{1/2},$$
$$V_2=abc(1-C-2P)^{1/2}.$$

Thus $V_1\neq V_2$,

and the two parallelepipeds cannot be transformed into each other by permuting the axes.

Before performing the reduction, or using the program that follows, it is necessary to define a reciprocal cell with right-handed indexing and a homogeneous vertex at the origin. An algorithm follows for doing this for a triclinic cell, provided that the same crystal is used for all the photographs. Since axial labelling may not be done till the precession photographs have been studied, the axes are first given provisional designations *m*, *n*, and *o* (the rotation axis), and the inter-axial angles named λ, (between *m* and *n*), μ, (between *n* and *o*), and ν, (between *o* and *m*).

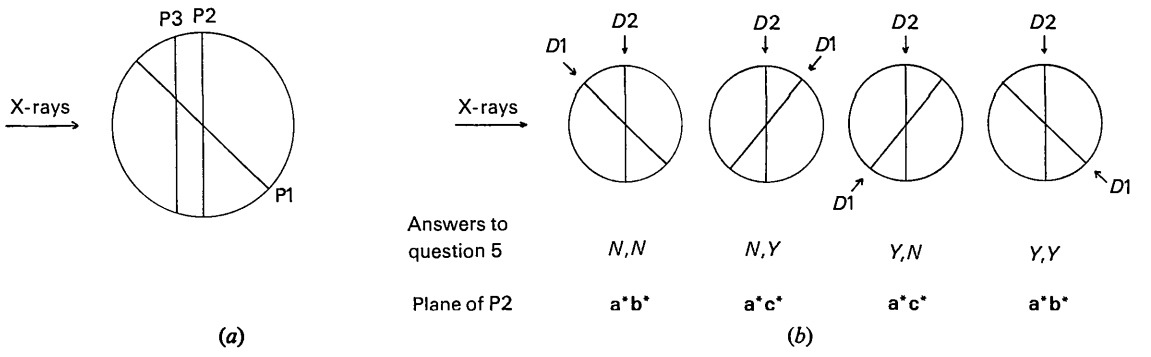

Fig. 1. (*a*) Three precession photographs showing relative positions of the films; **a*** is normal to the paper, and the positive direction extends toward the observer. (*b*) The four possible dial axis settings for the photographs P1, P2. The answers indicated for question 5 are those appropriate for an acute reciprocal cell. Axial orientation as in (*a*)

1. Determine the spacing along the rotation axis. One of the conventional labels can be given at choice to this axis, and in the treatment that follows this is assumed to be a; when one axis has been specified, the other labels cannot be assigned arbitrarily in a triclinic cell if the conditions above are to be met. Table 1 lists the changes needed in Table 2 if a different label is used.

2. On the zero-layer Weissenberg photograph assign provisional axial labels m^*, n^*, choosing a value for $\lambda^* \lesssim 90°$.

3. Transfer the crystal to the precession camera and align **o*** with the dial axis. Instructions for doing this for a triclinic crystal of undetermined lattice parameters, when the planes of the arcs make general angles with the X-ray beam, are available from the author.

Table 1. *Changes necessary in Table 2 consequent on the different labelling of the rotation axis*

	Rotation axis
a	Use the symbols as printed in Table 2: $a\ b\ c\ h\ k\ l\ \bar{h}\ \bar{k}\ \bar{l}$
b	Replace the symbols in line 1 above by: $b\ c\ a\ k\ l\ h\ \bar{k}\ \bar{l}\ \bar{h}$
c	Replace the symbols in line 1 above by: $c\ a\ b\ l\ h\ k\ \bar{l}\ \bar{h}\ \bar{k}$

Take three precession photographs, P1, P2, P3, in that order. Photographs P1 and P2 show the ($hk0$) and ($h0l$) nets, though not necessarily respectively, while for P3 the film has been advanced toward the crystal by one scaled reciprocal-lattice unit from the position for P2 [*cf.* Fig. 1(*a*)]. Record the dial readings $D1$, $D2$ for P1, P2, respectively.

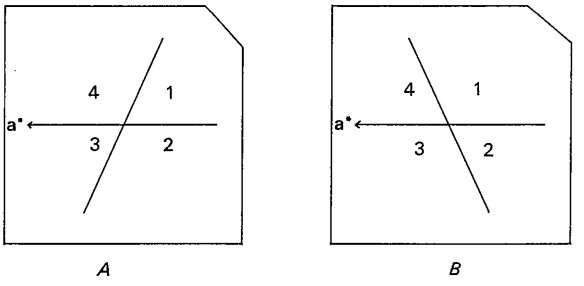

Fig. 2. Precession photographs showing axial lines and sector numbers.

4. Evaluate E, F, G, and H, thus:

$E = D2 - D1$

If E is positive $F = E$; otherwise $F = 360° + E$

If $F \lesssim 180°$ $G = F$; otherwise $G = 360° - F$

If $G \lesssim 90°$ $H = G$; otherwise $H = 180° - G$

Provisionally, set λ (α in this example) $= H$, *i.e.* to an angle $\lesssim 90°$. On P1, P2, measure the interaxial angles μ^*, ν^*, choosing for each a provisional value $\lesssim 90°$. With these provisional values, evaluate A, B, C, thus:

$$A = \cos\lambda \sin\mu^* \sin\nu^*$$
$$B = \cos\mu^* \cos\nu^* - \cos\lambda^*$$
$$C = \cos\mu^* \cos\nu^* + \cos\lambda^*$$

Either $A = -B$, in which case the reciprocal cell is *acute*,

or $A = +C$, in which case the reciprocal cell is *obtuse*.

5. Set down the true value for λ(α in this example).

(*a*) Is $G = \lambda$(*true* value)? Write Y/N for Yes/No

(*b*) Is $F > 180°$? Y/N

Fig. 2 and Table 2 then give the indexing for P1, P2, and P3. The method for deriving Table 2 follows from Fig. 1(*b*), and the answers indicated in that Figure to question 5 above can be obtained instantly by setting $D1 = 0°$. The rest of Table 2 can be constructed by setting one's right hand appropriately over the diagrams.

From the pattern of intensities on the precession photographs the corresponding patterns for the ($0kl$), ($1kl$), *etc.*, nets can be derived, and the various sectors

Table 2. *The indexing of the precession photographs*

		Photograph P2			Photograph P3	
Reciprocal cell type	Answers to question 5	Indexing	Type on Fig. 2 most like P2	Sector with both indices positive	Indexing	Spot with lowest indices and sector It lies in*
Acute	Y,Y or N,N	$hk0$	A	3	$hk\bar{1}$	$00\bar{1}$ 1
			B	4	$hk1$	001 4
	Y,N or N,Y	$h0l$	A	3	$h1l$	010 3
			B	4	$h\bar{1}l$	$0\bar{1}0$ 2
Obtuse	Y,Y or N,N	$hk0$	A	4	$hk1$	001 2
			B	3	$hk\bar{1}$	$00\bar{1}$ 3
	Y,N or N,Y	$h0l$	A	4	$h\bar{1}l$	$0\bar{1}0$ 4
			B	3	$h1l$	010 1

The corresponding data for photograph P1 can be found by interchanging the values for $D1$ and $D2$.

* The site of the spot may lie within the central blind area.

identified on the Weissenberg photographs which can then be indexed. On some Weissenberg photographs spots may generate lines that are sensibly straight, even though they are not axial lines. Such lines, if present, can be used to check the indexing, thus:

The position at which the rotation axis cuts the (*nkl*) reciprocal net can be found graphically. Draw the (**b***c*) net; a scale of 50 mm per reciprocal-lattice unit is convenient. Along **b***, **c**,* set off points *B*, *C*, at distances $-a^* \cos \gamma^*$, $-a$ *$\cos \beta^*$, respectively, from the origin, *O*. At points *B*, *C*, draw perpendiculars to **b***, **c***, and produce them to intersect at *R*. Draw *OR*, and extend this line, marking off distances from the origin equal to *OR*, 2*OR*, 3*OR*, *etc.*, and call the points at the ends of these vectors R_1, R_2, R_3, and so on. The point R_n is the position of intersection of the axis of rotation with the (*nkl*) net. The closer one of these points fall to one of the lines of the reciprocal net, the more nearly straight is the corresponding line of spots on the Wiessenberg photograph. Thus, in Fig. 3, R_3 is close to the line $b^*=2$, so that on the photograph of the (3*kl*) net the spots (32*l*) would form a (nearly) straight line. Such a line can have a constant positive value for *k* and/or *l* only if the reciprocal cell is obtuse, and a constant negative value if the cell is acute.

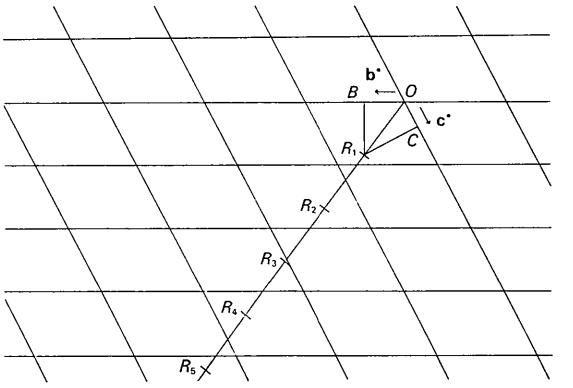

Fig. 3. Points of intersection of the rotation axis with successive nets in an obtuse reciprocal cell.

The predicition of spot positions

If the reciprocal axes *a**, *b**, *c**, are numbered respectively 1,2,3, and the film viewed in the orientation described above, then on both upper and lower halves of the film the axial numbers, expressed modulo 3, increase from right to left.

Let the axis with the lower number be *S**, and the one with the higher number be *T**, and the third reciprocal axis be *U**; thus the real axis, *U*, is the rotation axis. Let the interaxial angles be σ^* (between T^* and U^*), τ^* (between U^* and S^*), and υ^* (between S^* and T^*); let the unit translations along these axes be **s***, **t***, **u***, respectively, measured in reciprocal Ångström units (thus, for an *a* axis rotation $\mathbf{s}^* \equiv \mathbf{b}^* \simeq 1/\mathbf{b}$, *not* $\simeq \lambda/\mathbf{b}$). Table 3 relates these symbols to the conventional labels for each axis of rotation.

Table 3. *Dependence of the symbols S*, T*, U*, σ*, τ*, υ*, on the rotation axis*

Rotation axis	S^*	T^*	U^*	σ^*	τ^*	υ^*
a	b^*	c^*	a^*	β^*	γ^*	α^*
b	c^*	a^*	b^*	γ^*	α^*	β^*
c	a^*	b^*	c^*	α^*	β^*	γ^*

Following Buerger (1942*b*), let us define a system of cylindrical coordinates (ζ, r, φ), where ζ is the coordinate along the axis of the cylinder, and within each net *r* is the radial, φ the angular coordinate; both ζ and *r* are measured in reciprocal Ångström units. Also fol-

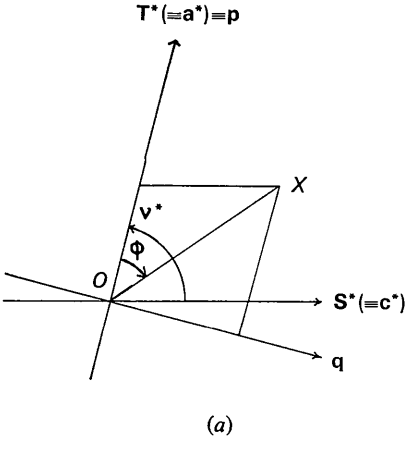

(*a*)

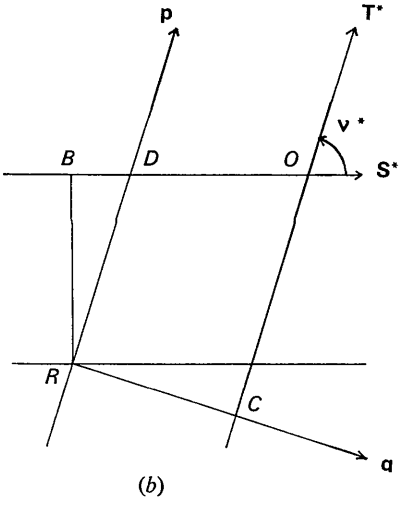

(*b*)

Fig. 4. (*a*) The relations between the axes of the various coordinate systems for the zero layer of a monoclinic cell rotated about **b**. (*b*) The relations between the axes of the various coordinate systems for the first layer of an acute triclinic reciprocal cell.

lowing Buerger (1942*a*) let us use film coordinates (x,z), expressed in mm, defining the position of a spot with respect to axes perpendicular to, and along the trace of the direct beam, respectively, and whose origin lies at the intersection of the trace with the left-hand edge of the film (not of the exposed area). Coordinate z increases from left to right; x is taken as positive on both upper and lower halves of the film. Then, on the upper half of a Wiessenberg photograph, taken on a camera such that the cassette moves 1 mm for each 2° of crystal rotation, and for a layer with equi-inclination angle eq, the film coordinates (x,z) are related to (r,φ) by the equations

$$x=\text{scf. } \sin^{-1}(r\,\lambda/2\cos\text{eq}),$$
$$z=x/2+\varphi/2-\varphi_0/2,$$

where scf is a scaling factor dependent on the curvature of the film, and φ_0 is the direction in reciprocal space corresponding to $z=0$. If C is the cassette radius and F the film thickness (both in mm), N the number of films in the pack and M the serial number of the film within the pack, with the film nearest the crystal as no. 1, then

$$\text{scf}=[C-(N-M)\times F]/C.$$

If on a film taken with a dial axis reading D_0 a spot of known indices has a measured z coordinate zz, and a calculated one, taking $\varphi_0=0$, of z_0, then, for another film for which the dial axis reading is D_n, the equation above for z becomes

$$z=x/2+\varphi/2+(D_0-\text{S1}\times D_n)/2+(zz-z_0).$$

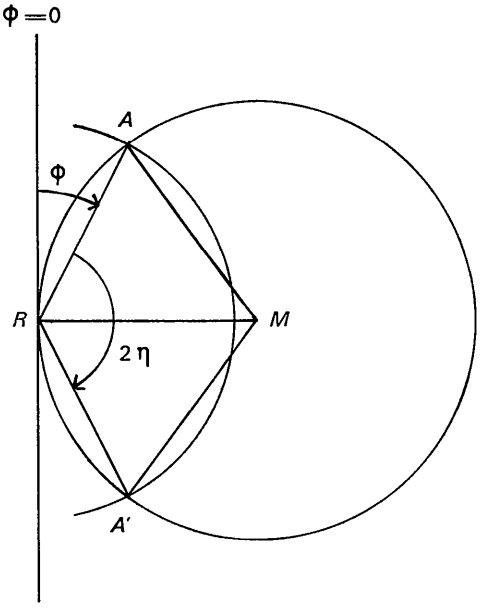

Fig. 5. The crystal rotation required between recording a reflexion on the upper and lower halves of a Weissenberg photograph.

To relate the system of cylindrical coordinates to the reciprocal axes we select an orthogonal system of axes (ζ,p,q), with ζ defined above, and $p=r\cos\varphi$, $q=r\sin\varphi$. Since the ζ axis and the rotation axis coincide, and because φ and υ increase in opposite senses, the axial systems (ζ,r,φ), and (ζ,p,q) are both left-handed. It is convenient to have the directions $(+\mathbf{T}^*)$, $(+\mathbf{p})$, and $(\varphi=0)$ parallel. On a zero-layer photograph these three axes coincide, and Fig. 4(*a*) shows the geometry for the reciprocal net of a monoclinic crystal rotated about b.

Let X be a reciprocal lattice point with indices $(j_t,0,j_s)$. Then in the system for the (p,q) net its coordinates in reciprocal Ångström units are:

$$p=j_s\,.\,s^*\,.\cos\upsilon^*+j_t\,.\,t^*$$
$$q=j_s\,.\,s^*\,.\sin\upsilon^*$$

The values for r and φ follow, and hence for x and z. However, in the case of an upper-layer photograph of a triclinic cell, the origin of the reciprocal net, and the intersection of the net with the rotation axis do not coincide. Fig. 4(*b*) shows this situation for the first layer of an acute triclinic cell. Point O is the origin of the net, while point R is the intersection of this net with the axis of rotation. On the Weissenberg photograph it is point R that forms the line $x=0$, and so must be the common origin of the (r,φ), and (p,q) nets. Provided the reciprocal cell has a homogeneous vertex at the origin, R will lie either in the sector between $+S^*$ and $+T^*$ (obtuse vertex), or between $-S^*$ and $-T^*$ (acute vertex). Then, if the coordinates of point 0 in the (p,q) system are (p_0,q_0), the coordinates in this system of the reciprocal-lattice point with indices (j_t,j_s) are $[(p+p_0),(q+q_0)]$, where p and q are given by the equations above; and

$$r=[(p+p_0)^2+(q+q_0)^2]^{1/2}.$$

The coordinates of point O are found thus: Point R lies at the intersection of lines through point C, perpendicular to $\mathbf{T}^*$; and through point B, perpendicular to $\mathbf{S}^*$. Now $OC=-u^*\,.\cos\sigma^*$, $OB=-u^*\,.\cos\tau^*$, and hence

$$p_0=u^*\,.\cos\sigma^*,$$
$$q_0=RC=[(OR)^2-(OC)^2]^{1/2}\times\text{sign},$$

where the positive value of the root is taken, and sign $=+1$ if the reciprocal cell is acute, -1 if it is obtuse. If (Buerger, 1942*c*) the angle between $\mathbf{U}$ and $\mathbf{U}^*=\varrho$, a little manipulation gives

$$q_0=u^*\,.\,(\sin^2\varrho-\cos^2\sigma^*)^{1/2}\times\text{sign}.$$

For the general case of an n-layer photograph, the values of p_0 and q_0 must be multiplied by n.

The analysis above is appropriate for only one half (assumed the top) of the Weissenberg photograph. However, each reciprocal-lattice point generates two Weissenberg spots; one when it enters, and one when

it leaves the sphere of reflexion. Fig. 5 shows the geometry; the arc AA' is the track of a reciprocal-lattice point rotated about R, and $RA=r$, and $RR=RM=MA$, the radius of the circle which the spehre of reflexion cuts in the n-layer net. Then

$$\cos\eta=[r^2/\{2\times(RR)^2\}]-1\ .$$

Thus, a reflexion generated at A will appear in the top half of the record with z-coordinate $=z_t$, corresponding to φ; and, after the crystal has been rotated by $2\times\eta$, the reflexion at A' will appear on the lower half of the film with z coordinate $=z_1$, corresponding to $(\varphi+2\times\eta)$; or, $z_1=z_t+\eta$.

A program written in FORTRAN IV for an ICL 1905 computer to perform the operations analysed above is available from the author.

References

AZAROFF, L. V. & BUERGER, M. J. (1958). *The Powder Method*, Ch. 11. New York: John Wiley.

BUERGER, M. J. (1942*a*). *X-ray Crystallography*, Ch 14. New York: John Wiley.

BUERGER, M. J. (1942*b*). *X-ray Crystallography*, pp. 135, 233. New York: John Wiley.

BUERGER, M. J. (1942*c*). *X-ray Crystallography*, p. 347. New York: John Wiley.

KENNARD, O., SPEAKMAN, J. C. & DONNAY, J. D. H. (1967). *Acta Cryst.* **22**, 445.

PEERDEMAN, A. F. & BIJVOET, J. M. (1956). *Acta Cryst.* **9**, 1012.

RAMASESHAN, S. (1964). *Advanced Methods of Crystallography*, p. 75. Edited by RAMACHANDRAN, G. N. London: Academic Press.

STOUT, G. H. & JENSEN, L. H. (1968). *X-ray Structure Determination*, p. 101. New York: Macmillan.

Acta Cryst. (1971). A**27**, 238

Anharmonic Non-Gaussian Contribution to the Debye–Waller Factor for NaCl

BY N. M. BUTT

Pakistan Institute of Nuclear Science and Technology, Rawalpindi, Pakistan

AND G. SOLT

Central Research Institute for Physics, Budapest 114, *P.O. Box* 49, *Hungary*

(*Received* 28 *August* 1970)

Measurement and theoretical estimate of the anharmonic non-quadratic contribution to the Debye–Waller factor for NaCl are reported. For the experiment the Mössbauer γ-ray diffraction technique was used to find the elastic diffracted intensity separated from the thermal diffuse scattering. The theoretical treatment makes use of the asymptotic form of the displacement correlation functions to give simple explicit expressions for the non-quadratic term. The role of the relevant lattice dynamical parameters is discussed. The deviation from the Gaussian form of the Debye–Waller factor is shown to be large enough to be observed, and the possibility of estimating the third-order anharmonic coupling constant from such a measurement is indicated.

Introduction

As is well known, the Debye–Waller factor governing the intensity of elastic scattering processes in a crystal defined as

$$f(\mathbf{k},T)=\langle e^{i\mathbf{ku}}\rangle_T$$

can generally be written in the cumulant expansion form

$$f(\mathbf{k}T)=\exp\{-\tfrac{1}{2}\langle(\mathbf{ku})^2\rangle_T+\tfrac{1}{24}[\langle(\mathbf{ku})^4\rangle_T-3\langle(\mathbf{ku})^2\rangle_T^2]+O(\mathbf{k}^6)\} \quad (1)$$

where $\mathbf{k}$ is the change in the wave-vector of the scattered quantum, $\mathbf{u}$ is the displacement of the scattering atom from the lattice equilibrium position and the bracket means thermal averaging over the dynamical states of the crystal. If the lattice sites have inversion symmetry, the odd powers in (1) are absent. Higher than fourth-order terms will be neglected here.

The physical information contained in the Debye–Waller factor is particularly clear if the dynamics of the lattice can be described entirely by using the harmonic approximation, when only the quadratic term appears in the exponent and one has a Gaussian distribution in $\mathbf{k}$ with a width determined by the mean-square displacement of the atoms. It was suggested a long time ago that careful investigation of the Debye–Waller factor can be a very useful tool to study anharmonic properties of crystals. The anharmonic coupling leads to a change in the mean-square displacement as compared with the harmonic value, and also gives rise to the quartic (and higher-order) terms in (1). The presence of the quartic term representing the deviation from the Gaussian behaviour is an in-